PHYSICAL REVIEW D VOLUME 3, NUMBER 1 1 JANUARY 1971

Momentum Spectrum of Hadronic Secondaries in the Multiperipheral Model*

CARLETON E. DETAR†
Lawrence Radiation Laboratory, University of California, Berkeley, California 94720
(Received 17 August 1970)

Motivated by a simplified multiperipheral model, we formulate a general qualitative description of the momentum spectrum of secondaries, resulting from a collision of two hadrons at high energies. Arguing from two fundamental multiperipheral concepts, (a) that transverse momenta are limited and (b) that distant particles on the multiperipheral chain are uncorrelated, we predict that at sufficiently high incident energies, the momentum spectrum of particle X in the reaction $a+b \to X+$anything, when presented in the variables $p_\perp$ and $y=\sinh^{-1}[p_{\parallel}/(p_\perp^2+m_X^2)^{1/2}]$, develops a central plateau in the y dependence, which elongates and flattens to a value that is normalized by the total cross section as the incident energy increases. Moreover, it is shown that the resultant particle density distribution is consistent with the hypothesis of limiting fragmentation. We contrast this description with the predictions of the two-fireball model, the isobar-pionization model, and the statistical thermodynamical model.

I. INTRODUCTION

INTEREST in multiperipheral models for particle production has revived recently in theoretical efforts to incorporate multiparticle unitarity into a bootstrap program[1–5] and in phenomenological work in fitting production data at accelerator energies.[6] They are attractive models for studying particle production at high energies, since bootstrap constraints can provide a measure of uniqueness in the construction of the models, and they are ideally suited for extrapolating phenomenological studies to higher energies.

The variety of multiperipheral models in current use is considerable. The pion-exchange model of ABFST[7] is still of great theoretical interest.[4,5] A version of the Bethe-Salpeter model has been applied to multiparticle production.[8] The multi-Regge exchange model[9] has enjoyed considerable success in the study of reactions with three-body final states[10] and the CLA model[6] has performed remarkably well in fitting production data.[6,11]

These models have the following common features. (a) The distribution in transverse momentum is limited. (b) They describe particle production in terms of a linear chain of repeating links (with incident particles attached to the ends), along which only "neighboring" particle momenta are correlated. For present purposes we shall say two particles are neighboring if their invariant mass—more specifically, the Lorentz boost parameter that relates their rest frames—is less than a prescribed constant value. Alternatively, one could define a neighboring particle in terms of the number of intervening particles on the chain. In most models both definitions are closely related, and both can serve as a basis for constructing a Fredholm equation for summing multiparticle contributions to unitarity equations. However, there is an advantage for us in the first definition in that it relates more directly to the momentum spectrum. Furthermore, as a hypothesis it has the advantage of experimental verifiability, since it does not require that observed particles be ranked according to an arbitrary sequence on a chain. By a lack of correlation between two particles we simply mean that the functional dependence of the production cross section upon the momenta and other quantum numbers of the particles be factorizable. In particular, a power behavior in the subenergy $s_{ij}=(P_i+P_j)^2$ is factorizable in the momenta, provided that s_{ij} greatly exceeds the squared transverse momenta and masses of the particles. This follows from the result, when $p_{\parallel j} \gg p_{\parallel i}$ (see the Appendix), that

$$s_{ij}=p_{\parallel j}/p_{\parallel i}(p_{\perp j}^2+m_j^2). \tag{1.1}$$

Since the subenergy factors in its momentum dependence, any amplitude which incorporates simple power behavior at large adjacent-particle subenergies (Regge behavior, elementary particle exchange) with a factored coefficient provides for a dynamical decoupling of particle momenta at high invariant masses. If the particles are not adjacent on the chain, the large number of intervening particles (with direct factorization at low subenergies as, for example, in the ABFST[7] model) or factorization at large subenergies (or both), results in decoupling at large invariant masses in most models. We shall demonstrate with a simple model that there is reason to expect that dynamical decoupling survives kinematical constraints, provided transverse momenta are small, and carries over into the production

* Work supported in part by the U. S. Atomic Energy Commission.
† Present address: Massachusetts Institute of Technology, Cambridge, Mass. 02140.
[1] G. F. Chew and A. Pignotti, Phys. Rev. 176, 2112 (1968); Phys. Rev. Letters 19, 614 (1967).
[2] G. F. Chew, M. Goldberger, and F. Low, Phys. Rev. Letters 22, 208 (1969).
[3] I. G. Halliday and L. M. Saunders, Nuovo Cimento 60A, 115 (1969); 60A, 494 (1969).
[4] G. F. Chew, Terence Rogers, and Dale R. Snider, Phys. Rev. D 2, 765 (1970).
[5] G. F. Chew and Dale R. Snider, Phys. Rev. D 1, 3453 (1970).
[6] Chan Hong Mo, J. Łoskiewicz, and W. W. M. Allison, Nuovo Cimento 57, 93 (1968).
[7] L. Bertocchi, S. Fubini, and M. Tonin, Nuovo Cimento 25, 626 (1962); D. Amati, A. Stanghellini, and S. Fubini, *ibid.* 26, 896 (1962).
[8] V. N. Akimov, D. S. Chernavskii, I. M. Dremin, and I. I. Roysen, Nucl. Phys. B14, 285 (1969), and references therein.
[9] See Ref. 1 and other references contained therein.
[10] Edmond L. Berger, Phys. Rev. 179, 1567 (1969), and references therein.
[11] G. Ranft, Nuovo Cimento 58A, 425 (1968); E. Plahte and R. G. Roberts, *ibid.* 60A, 33 (1969).

cross section itself. At the end of Sec. III we show that the cross section for producing two particles in conjunction with anything else should have the same power behavior at large subenergies as does the total cross section in the total energy (and therefore decouples). Therefore, for the present discussion, we shall adopt the above two conditions as the defining criteria of multiperipheralism.

We shall be primarily concerned here with general qualitative features within multiperipheral models of the spectrum $d^2\sigma/dp_\perp dp_{11}$ for the momentum of particle X in the process $a+b\to X+$anything. In particular we shall study the evolution of the spectrum with increasing energy, as contrasted with the predictions of the two-fireball model and the isobar-pionization model. Of course, a detailed prediction of the spectrum requires a careful study within a particular model. Caneschi and Pignotti[12] obtained a quite satisfactory fit to data for the reactions $pp\to p+$anything and $pp\to\pi^\pm+$anything within the context of the multi-Regge model. Using a similar model, Silverman and Tan[13] fitted data for the low-energy part of the missing-mass spectrum in $\pi^-p\to p+\mathrm{MM}$.

However, a comprehensive analysis of the common features of spectra predicted by multiperipheral models has yet to be accomplished. This work is a contribution to such an effort. We shall motivate our discussion of the secondary momentum spectrum with a simplified multiperipheral model. Nevertheless, we shall deal with the deficiencies of this model, and in so doing, shall avoid adopting a specific model; rather, we shall attempt to identify the broad features of the spectrum, which any multiperipheral model should produce.

In Sec. II we introduce a particularly useful set of variables in which to represent the momentum spectrum. They are the transverse momentum $p_\perp$ and a longitudinal boost variable[14,15]

$$y=\sinh^{-1}[p_{11\mathrm{lab}}/(p_\perp^2+m^2)^{1/2}].$$

We reformulate the Chew-Pignotti multi-Regge model in terms of these variables in Sec. III and produce a simplified spectrum with the model. Following a critique of the assumptions of the Chew-Pignotti model we discuss in Sec. IV modifications that would bring the model more nearly in accordance with reality, and estimate the attendant modifications to the simplified spectra. The reader may, if he wishes, omit Secs. III and IV, since the concluding sections are self-contained. In Sec. V we argue on the basis of our general criterion for multiperipheral models that at sufficiently high energies, the particle density (the production spectrum

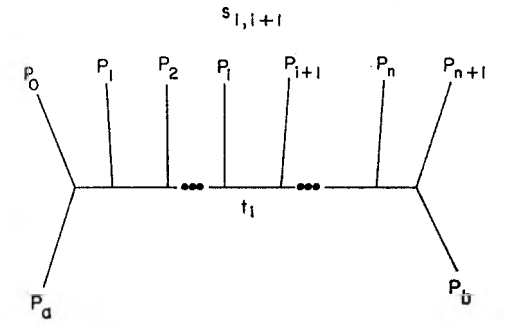

FIG. 1. Diagram for the production of n particles, showing the definition of the subenergies and momentum transfers.

divided by the total cross section) for particle X in the process $a+b\to X+$anything should approach the form

$$(\sigma_{ab}{}^{\mathrm{tot}})^{-1}\frac{d^2\sigma_{ab}{}^X}{dp_\perp dy}=\begin{cases}A_X(p_\perp,y) & \text{for } y<\Delta\\ f_X(p_\perp) & \text{for } \Delta<y<Y-\Delta\\ B_X(p_\perp,Y-y) & \text{for } Y-\Delta<y,\end{cases}\qquad(1.2)$$

where $s=m_am_be^Y$ for large s, A_X depends only upon particles a and X, and B_X depends only upon b and X. The constant Δ is chosen to be appropriately large and is related, roughly speaking, to the correlation distance in the Lorentz boost parameter y. The function f_X is universal, depending only upon the particle X.

Finally, in Sec. VI we contrast the predictions of the multiperipheral model with those of the two-fireball model, the isobar-pionization model, and the statistical thermodynamical model.

II. KINEMATICAL VARIABLES

To simplify the discussion of the momentum spectrum of secondaries, we have found a useful set of kinematical variables, which emphasize the different roles of the longitudinal and transverse directions.

We view the process (Fig. 1)

$$a+b\to 0+1+\cdots+n+(n+1)\qquad(2.1)$$

in the laboratory system, in which particle a is at rest and particle b moves along the positive z axis. We may write

$$\begin{aligned}P_a&=(m_a,0,0,0),\\ P_b&=(m_b\cosh Y,0,0,m_b\sinh Y),\\ P_i&=(w_i\cosh y_i,p_{ix},p_{iy},w_i\sinh y_i),\end{aligned}\qquad(2.2)$$

where

$$w_i=(m_i^2+p_{1i}^2)^{\frac{1}{2}},\quad p_{1i}=|\mathbf{p}_{1i}|,\quad \mathbf{p}_{1i}=(p_{ix},p_{iy}).$$

We call the variable y_i the longitudinal boost. It specifies the z boost that relates the rest frame of particle a to the frame in which particle i moves in a direction perpendicular to the beam.

[12] L. Caneschi and A. Pignotti, Phys. Rev. Letters **22**, 1219 (1969).
[13] Dennis Silverman and Chung-I Tan, Phys. Rev. D **2**, 233 (1970).
[14] Feynman (Ref. 15) has mentioned that this variable would be useful.
[15] R. P. Feynman, Phys. Rev. Letters **23**, 1415 (1969); in *High Energy Collisions* (Gordon and Breach, New York, 1969), p. 237.

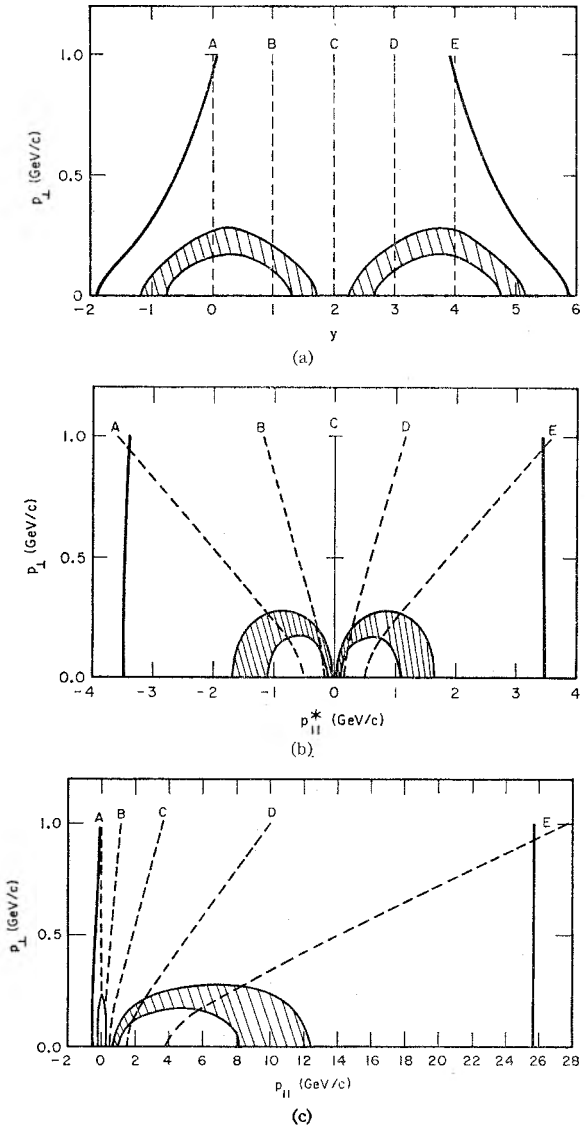

FIG. 2. Comparison of the longitudinal boost plot (a) with the Peyrou plot in the center-of-mass frame (b) and lab frame (c). The phase-space boundary is indicated with a heavy line for the process $pp \to \pi+$ anything with beam momentum 25.6 GeV/c (m_p sinh4). The shaded band denotes the position of pions that result from the process $pp \to \Delta_{1236}\Delta_{1236}$ in the near forward direction. The band corresponds to a mass width of 120 MeV.

The phase space in terms of these variables is simply

$$d\Phi_n \equiv \prod_{i=0}^{n+1} \frac{d^3p_i}{E_i}\delta^4\Big(\sum_{i=0}^{n+1} P_i - P_a - P_b\Big)$$

$$= \tfrac{1}{2}\prod_{i=0}^{n+1} d^2\mathbf{p}_{\perp i}dy_i\delta^2\Big(\sum_{i=0}^{n+1}\mathbf{p}_{\perp i}\Big)\delta\Big(\sum_{i=0}^{n+1} w_i e^{y_i} - m_a - m_b e^{Y}\Big)$$

$$\times\delta\Big(\sum_{i=0}^{n+1} w_i e^{-y_i} - m_a - m_b e^{-Y}\Big). \quad (2.3)$$

The latter two δ functions are obtained by rewriting the conventional constraints on the energy and z components of the momenta in the form

$$\tfrac{1}{2}\delta\Big(\sum(E_i+P_{iz}) - (E_a+P_{az}) - (E_b+P_{bz})\Big)$$
$$\times\delta\Big(\sum(E_i-P_{iz}) - (E_a-P_{az}) - (E_b-P_{bz})\Big). \quad (2.4)$$

In the Appendix we relate these variables to the familiar invariants $s_{i,i+1}$, t_i, etc. In particular, for large $s = (P_a+P_b)^2$, s (therefore the beam momentum) is exponentially related to Y:

$$s = m_a^2 + m_b^2 + 2m_a m_b \cosh Y \sim m_a m_b e^{Y}. \quad (2.5)$$

There are several advantages to presenting distributions in the longitudinal boost variables y and $p_\perp$ rather than in a Peyrou plot ($p_\parallel$ vs $p_\perp$). (a) All longitudinally moving frames are put on equal footing, since a linear scale change in y connects them all. There is complete symmetry between the rest frame of the projectile and the lab frame in the plot. (b) We will argue below that the distribution in the variable y is constant for the part of the spectrum that arises from positions of the multiperipheral chain that are sufficiently distant from the ends. Hence, on the average, particles will be uniformly spaced in the variable y for $\Delta < y < Y - \Delta$, where Δ is suitably chosen. (c) The subenergy of a particle pair depends upon the relative spacing of points in y. The decay spectrum of a resonance has the same shape anywhere in the plot for any total energy, provided the transverse momentum of the resonance is the same. Thus the variable y would be a natural choice for studying models that emphasize the role of final state resonances at arbitrary longitudinal momenta. (d) For $p_{\parallel\text{lab}} \gg p_\perp \gg m$, $y = \ln(2/\tan\theta_{\text{lab}})$, thereby providing a simple connection with the Lindern plot ($d\sigma/d\log\tan\theta$).[16] In particular, a measurement of the production spectrum at fixed angle and large momentum corresponds to a measurement at fixed y and large $p_\perp$.

Figure 2 illustrates the correspondence between lab momenta, center-of-mass momenta, and the longitudinal boost variable for $pp \to \pi+$anything at 25.6 GeV/c (corresponding to a value of $Y = 4$). The absolute kinematical limits on the longitudinal boosts may be deduced from the last two δ functions in (2.3). These are

$$w_i/m_a < e^{y_1} < e^{Y} m_b/w_i, \quad (2.6)$$

shown as bold lines in Fig. 2. Note that the c.m. Peyrou plot and the lab-frame plot concentrate a large part of the spectrum in y into a small region about $p_\parallel = 0$ (as is expected from the Jacobian $dy = dp_\parallel/E$). Also shown in Fig. 2 is the location in this plot of pions that would result from the process $pp \to \Delta(1236)\,\Delta(1236)$ for small $p_{1\Delta}$. Note the energy-dependent elongation of the spectrum in the momentum-space plot. Although the spectrum $d^2\sigma/dydp_\perp$ is easily related to the spectrum $d^2\sigma/dp_\parallel dp_\perp$, the spectrum $d\sigma/dy$, obtained by integrating with y fixed, obviously gives a quite different

[16] L. v. Lindern, Nuovo Cimento 5, 491 (1957).

representation of the production mechanism from the spectrum $d\sigma/dp_{\parallel}$, obtained by integrating with $p_{\parallel}$ fixed.

Another currently popular variable, $x=p_{\parallel \text{c.m.}}/p_{a,\text{c.m.}}$, was introduced by Feynman.[15] This variable has the attractive feature that the spectrum lies within the fixed limits $-1\leq x\leq 1$ as the energy increases. For finite x and sufficiently large energies, the variables x and y are logarithmically related:

$$x=\begin{cases}(w_i/m_b)e^{y-Y} & \text{for} \quad Y/2\ll y<Y+\ln(m_b/w_i)\\ -(w_i/m_a)e^{-y} & \text{for} \quad -\ln(m_a/w_i)<y\ll Y/2.\end{cases} \tag{2.7}$$

Hence, a distribution that is limiting in x for $x \gtrsim -x_{a,\min}$ and $x>x_{b,\min}$ is limiting in y for $y \gtrsim y_{a,\min}$ and $y>Y-y_{b,\min}$ for the corresponding $y_{a,\min}$, $y_{b,\min}$. In *either* variable the existence of a limiting distribution can be checked by superposing the appropriate part of the distribution at various energies without a scale change.

From the standpoint of most models with limiting fragmentation that predict divergent multiplicities, the variable x suffers from the property that the predicted spectrum $d^2\sigma/dxdp_{\perp}$ develops a sharp peak at or near $x=0$, which becomes sharper with increasing energy. This difficulty can be circumvented by using the technique of Bali *et al.*,[17] writing the cross section as

$$d^2\sigma/dp_{\parallel}dp_{\perp}=f(p_{\perp},x,s)/E, \tag{2.8}$$

where E is the energy of the observed particle, and studying the behavior of f as s is increased. However, it would be sensible to take advantage of the high statistical precision at "wee"[15] x ($x\lesssim w_i/\sqrt{s}$) and present the data on an expanded scale. For this purpose Feynman suggested an alternative variable equivalent to the variable y. For the reasons outlined above, we therefore propose that this variable be used for the entire spectrum.

III. SIMPLE MODELS

A. Chew-Pignotti Model

To establish a heuristic foundation for the discussion, we shall calculate the secondary momentum spectrum in a simplified multiperipheral model. We consider first a model equivalent to that of Chew and Pignotti[1] in simplicity. The model assumes that subenergies are all very large ("strong-ordering limit") and that the cross section for producing n particles is

$$\sigma_n\propto e^{-Y}\int g^{2n}\prod_{i=1}^{n+1}(s_{i,i+1})^{2\alpha}d\Phi_n. \tag{3.1}$$

In the strong-ordering limit,[18]

$$E_i\gg E_{i-1}, \quad E_i\gg w_i, \tag{3.2}$$

and the last two δ functions in the phase space (2.3) may be approximated by

$$e^{-Y}/m_am_b\delta(y_0-x_a)\delta(Y-x_b-y_{n+1}), \tag{3.3}$$

where

$$x_a=\ln(w_0/m_a) \quad \text{for} \quad x_b=\ln(w_{n+1}/m_b). \tag{3.4}$$

In this same limit the subenergies become (see the Appendix)

$$s_{i-1,i}\equiv(P_i+P_{i-1})^2\approx w_{i-1}w_ie^{z_i}, \tag{3.5}$$

where

$$z_i=y_i-y_{i-1}.$$

Changing variables and integrating y_0, we obtain a vastly simplified phase space analogous to that of Chew and Pignotti:

$$d\Phi_n\approx\frac{e^{-Y}}{2m_am_b}\prod_{i=0}^{n+1}d^3\mathbf{p}_{\perp i}\delta^2\Big(\sum_{i=0}^{n+1}\mathbf{p}_{\perp i}\Big)\times\prod_{i=1}^{n+1}dz_i\delta\Big(X-\sum_{i=1}^{n+1}z_i\Big), \tag{3.6}$$

where

$$X=Y-x_a-x_b,$$

and the lower bound on z_i is, roughly speaking,

$$z_i\gtrsim-(x_i+x_{i-1}), \quad \text{where } x_i=\ln(w_i/m_i). \tag{3.7}$$

The strong-ordering approximation is not realistic for the large bulk of production events. One obvious drawback is that as far as the process $a+b\to 0+(n+1)$ is concerned it describes only approximately elastic scattering, because the produced particles 1, 2, ..., n carry off a vanishing fraction of the total energy. Nevertheless, the enormous simplification obtained permits us to draw some useful conclusions. We shall later estimate the modifications necessary for a more rigorous treatment.

There are two important simplifying features of the strong ordering approximation. (a) The longitudinal momentum and cluster energy $s_{0i}\equiv(\sum_{j=0}^{i}P_j)^2$ are related to the variables in a simple way:

$$s_{0i}\approx 2m_ap_{\parallel i}\approx m_aw_ie^{y_i}. \tag{3.8}$$

(b) The phase space can be cast in a recursive form, making it a suitable basis for constructing an integral equation. We shall not demonstrate the last statement, but shall draw upon the results of the completely analogous treatment with the conventional invariants s_{0i} and t_i.[2,19]

We make the further kinematical simplification that transverse momenta may be ignored. Then $w_i\approx m_i$ and the lower bound on z_i is about 0. If for notational convenience we put $m_a=m_0$ and $m_b=m_{n+1}$, we obtain for σ_n the expression

$$\sigma_n\propto e^{-Y}g^{2n}e^{Y(2\alpha-1)}\int\prod_{i=1}^{n+1}dz_i\delta\Big(Y-\sum_{i=1}^{n+1}z_i\Big)\propto g^{2n}e^{Y(2\alpha-2)}Y^n/n!, \tag{3.9}$$

[17] N. F. Bali, Lowell S. Brown, R. D. Peccei, and A. Pignotti, Phys. Rev. Letters **25**, 557 (1970).

[18] F. Zachariasen and G. Zweig, Phys. Rev. **160**, 1326 (1967).

[19] Marvin L. Goldberger, Chung-I Tan, and Jiunn-Ming Wang, Phys. Rev. **184**, 1920 (1969).

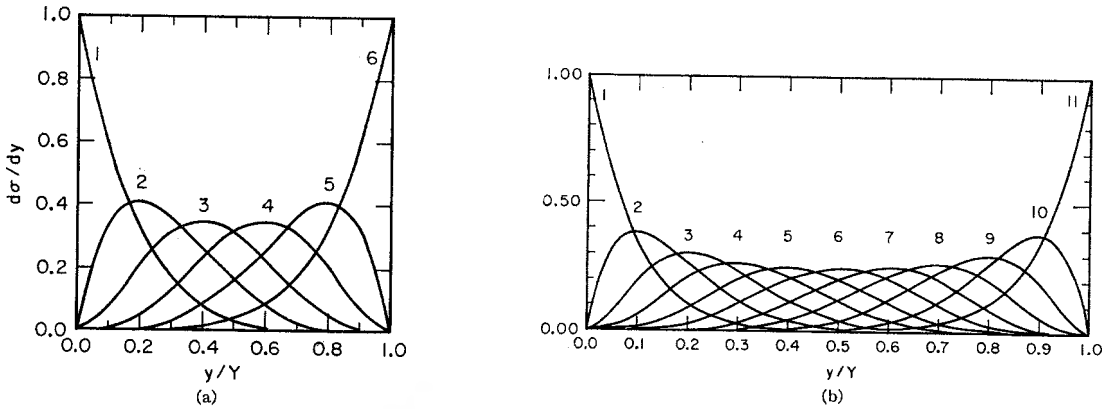

FIG. 3. Distribution in longitudinal momentum of the ith produced particle in a simplified Chew-Pignotti model; $d\sigma_i/dy$ for the ith particle is given in arbitrary units and y/Y is proportional to $\log p_{\parallel}$ (see text). Distributions are shown for (a) six and (b) eleven produced particles.

and the total cross section is simply

$$\sigma_{\text{tot}}=\sum_{n=0}^{\infty}\sigma_n\propto\exp[Y(2\alpha-2+g^2)]. \tag{3.10}$$

Chew and Pignotti put $2\alpha-1+g^2=1$ to obtain a constant total cross section. For the remainder of this section we shall assume that the total cross section is asymptotically constant.

The distribution in $\ln(p_{\parallel i}/m_i)\approx y_i$ for the n-particle production cross section at the energy e^Y may be obtained by fixing $y_i=\sum_{j=1}^{i}z_j$ in the phase-space integration above. Thus

$$\frac{d\sigma_{n,i}}{dy}=e^{Y(2\alpha-2)}g^{2n}\int\prod_{j=1}^{n+1}dz_j\delta(Y-\sum_{i=1}^{n+1}z_j)\times\delta(y-\sum_{j=1}^{i}z_j), \tag{3.11}$$

$$\frac{d\sigma_{n,i}(Y,y)}{dy}=e^{Y(2\alpha-2)}g^{2n}\frac{y^{i-1}}{(i-1)!}\frac{(Y-y)^{n-i}}{(n-i)!}.$$

This distribution is illustrated in Fig. 3 for $n=6$ and 11 and has the following interesting properties. (a) The maxima occur at regular intervals in y at $y/Y=(i-1)/n$. (b) The distributions for the central part of the chain are approximately equivalent under translation. This effect improves as n is increased. (c) The distributions are well confined in y_i. Since the invariant mass of particles 0 through i is related exponentially to y_i through Eq. (3.8), Fig. 3 can also be regarded as a distribution in the logarithm of the invariant mass of groups of particles. The distributions give the appearance of diffuse resonances whose masses grow exponentially with multiplicity.[20] If we lump together the distribution for all particles produced along the chain, we obtain the spectrum for producing one particle in conjunction with $n-1$ others. It is a *flat* distribution in y,

$$\frac{d\sigma_n}{dy}=\sum_{i=1}^{n}\frac{d\sigma_{n,i}(Y,y)}{dy}=e^{Y(2\alpha-2)}g^{2n}\frac{Y^{n-1}}{(n-1)!}. \tag{3.12}$$

The "inclusive"[15] spectrum is obtained by summing over n, and is also constant in y. The average multiplicity is obtained from the Poisson distribution (3.9) and is

$$\langle n\rangle=g^2Y. \tag{3.13}$$

The average spacing of the particles in y is therefore constant, independent of the total energy:

$$\langle\Delta y\rangle=Y/\langle n\rangle=1/g^2, \tag{3.14}$$

since the spacing is uniform along the chain. These results are all well-known consequences of the multiperipheral model.[7]

Suppose a model of particle production allowed a particle of type X to appear only at every other position on the chain. The spectrum for particle X would no longer be a constant as indicated in Eq. (3.12) but would oscillate.[21] The central part of the spectrum would have

TABLE I. Correlation fraction F_{ij}, giving a measure of the correlation in the Chew-Pignotti model between produced particles i and j on the multiperipheral chain, when six particles are produced.

i \ j	1	2	3	4	5	6
1	...	0.124	0.030	0.013	0.006	0.002
2		...	0.164	0.043	0.016	0.006
3			...	0.176	0.043	0.013
4				...	0.164	0.030
5					...	0.124
6						...

[20] Since the width and decay multiplicity of the mass enhancements depend on the total number of produced particles, one would presumably have to consider an event with average multiplicity in order to attach any significance to the mass enhancement as a resonance.

[21] I am indebted to W. R. Frazer for calling this possibility to my attention.

TABLE II. Correlation fraction F_{ij} for the production of eleven particles.

i \ j	1	2	3	4	5	6	7	8	9	10	11
1	···	0.156	0.041	0.021	0.013	0.009	0.006	0.004	0.003	0.002	0.001
2		···	0.199	0.063	0.033	0.020	0.012	0.008	0.005	0.003	0.002
3			···	0.230	0.080	0.042	0.025	0.015	0.009	0.005	0.003
4				···	0.247	0.089	0.046	0.026	0.015	0.008	0.004
5					···	0.255	0.092	0.046	0.025	0.012	0.006
6						···	0.255	0.089	0.042	0.020	0.009
7							···	0.247	0.080	0.033	0.013
8								···	0.230	0.063	0.021
9									···	0.199	0.041
10										···	0.156
11											···

a period of $Y/\frac{1}{2}n$. If we sum (3.12) over all multiplicities, we obviously obtain a flat distribution. However, if we omitted every other particle in the sum, the resultant distribution would be neither constant nor periodic, but could be rather lumpy. In an average sense, however, it would be a constant in y. The amplitude of oscillation depends on the sharpness of the localization of particles from a given position on the chain. The more localized they are, the more pronounced the oscillation. In the critique of the strong-ordering approximation in Sec. IV, we will conclude that in a more realistic model overlapping of longitudinal momenta is rather common. Hence the contribution from a given position on the chain is probably rather less concentrated in reality than Fig. 3 would suggest, and the net single-particle spectrum obtained by selecting every other particle in the model above is smoother than might be expected.

One of our criteria of multiperipheralism is that distant particles on the multiperipheral chain decouple. Although dynamical decoupling is easily achieved in practice by requiring that the amplitude factor in its momentum dependence, it is interesting to ask whether the kinematical constraint of energy and momentum conservation would permit a real decoupling of the momenta of produced particles.

Such kinematical correlations could conceivably be strong when the energies of particles are of comparable magnitude. However, it is a surprising consequence of the strong-ordering assumption that a kinematical decoupling takes place. To demonstrate this effect with the cross section (3.1), we have calculated a quantity, which we call the "correlation fraction," which gives a measure of the degree to which the longitudinal momenta of two particles on the chain, particles i and j, are correlated. We first calculate the joint distribution $d^2\sigma_{n;i,j}/dy_i dy_j$ from Eq. (3.9),

$$\frac{d^2\sigma_{n;i,j}}{dy_i dy_j} = e^{Y(\alpha-2)} g^{2n} \frac{(y_i)^{i-1}}{(i-1)!} \times \frac{(y_j-y_i)^{j-i-1}}{(j-i-1)!} \frac{(Y-y_j)^{n-j}}{(n-j)!} \quad \text{for } j>i \text{ and } Y>y_j>y_i>0. \quad (3.15)$$

For $y_j<y_i$ the distribution vanishes. If the momenta are uncorrelated, then

$$\frac{1}{\sigma_n}\frac{d^2\sigma_{n;ij}}{dy_i dy_j} = \frac{1}{\sigma_n^2}\frac{d\sigma_{n,i}}{dy_i}\frac{d\sigma_{n,j}}{dy_j}. \quad (3.16)$$

If we compare Eq. (3.15) with Eq. (3.11), it is obvious that this condition is not satisfied exactly. However, the relation is approximately correct. Let L_{ij} and R_{ij} denote, respectively, the left- and right-hand sides of Eq. (3.16). As a measure of their equality we calculate the fraction

$$F_{ij} = \int\int (L_{ij}-R_{ij})^2 \Big/ \left(\left| \int\int L_{ij}^2 \right|^{1/2} + \left| \int\int R_{ij}^2 \right|^{1/2} \right)^2. \quad (3.17)$$

From the Cauchy-Schwartz triangle inequality, it can be shown that

$$0 \le F_{ij} \le 1. \quad (3.18)$$

If $L_{ij}=R_{ij}$ everywhere, then $F_{ij}=0$, and the dependence on y_i and y_j is not correlated. When $F_{ij}\approx 1$, the dependence is strongly correlated. In Tables I and II we give the values of F_{ij} for $n=6$ and 11. Note that more distant particles are indeed less strongly correlated. Because of the localization of the spectra of Fig. 3, a decoupling of particles widely separated in rank on the chain is equivalent to a decoupling of pairs of particles with large invariant masses.

B. Model with Nonconstant Total Cross Section

We now consider a somewhat more sophisticated model, which admits a general energy dependence for the total cross section, while keeping the strong-ordering approximation and the approximation of ignoring transverse momenta. We take as a model for the square of the production amplitude, the factorized expression

$$|A_{ab}{}^n|^2 \propto G_a K(z_1) g^2 K(z_2) g^2 \cdots K(z_n) G_b, \quad (3.18')$$

where $K(z)$ may be thought of as the square of a propagator and g^2, the square of a vertex. They can be matrices in the channel indices. With such a model, one

may determine the total cross section

$$\sigma_{ab}=\sum_n \int d\Phi_n |A_{ab}{}^n|^2 \tag{3.19}$$

by means of an integral equation. This procedure has been discussed in considerable detail.[2] For our model, we have the following vastly simplified equations:

$$B_a(Y)=\int B_a(y)g^2K(z)\delta(Y-y-z)dydz+G_aK(Y),$$
$$\sigma_{ab}(Y)=e^{-Y}B_a(Y)G_b. \tag{3.20}$$

It is easy to verify by iterating (3.20) that σ_{ab} is given by (3.19) with the simplified phase space of (3.9).

We want to derive an expression for the spectrum in $\ln(p_{11}/m)\approx y$ for the production of one particle in conjunction with anything else. As before, the distribution $d\sigma_{ab}/dy$ is obtained by undoing the integration in the variable y in the total cross section. Keeping in mind that the cross section for producing n particles $\sigma_{ab}{}^n$ must be weighted by n in the inclusive spectrum, we see that we obtain $d\sigma_{ab}/dy$ by removing the integration over y in the expression

$$\int \frac{d\sigma_{ab}}{dy}dy=\sigma_{ab}{}^1+2\sigma_{ab}{}^2+3\sigma_{ab}{}^3+\cdots=\langle n\rangle\sigma_{ab}, \tag{3.21}$$

where $\langle n\rangle$ is the average multiplicity of the observed *produced* particle per event and σ_{ab} is the production cross section. Equation (3.21) may be written formally as

$$G_aKg^2KG_b+2G_aKg^2Kg^2KG_b+3G_aKg^2Kg^2Kg^2KG_b+\cdots. \tag{3.22}$$

Since

$$B_a=G_aK+G_aKg^2K+G_aKg^2Kg^2K+\cdots, \tag{3.23}$$

we see that

$$\langle n\rangle\sigma_{ab}=B_ag^2B_b. \tag{3.24}$$

More explicitly,

$$\langle n\rangle\sigma_{ab}=e^{-Y}\int B_a(y)g^2B_b(y')dydy'\delta(Y-y-y'). \tag{3.25}$$

Undoing the integration over y, we get, finally,[22,23]

$$\frac{d\sigma_{ab}(Y,y)}{dy}=e^{-Y}B_a(y)g^2B_b(Y-y). \tag{3.26}$$

(Note that the total area is $\langle n\rangle\sigma_{ab}$, as it should be.)

In general, $\langle n\rangle$ should be replaced by the multiplicity of the observed particle type, and g^2 on the right-hand side should correspond to that vertex, which emits the type of particle in question.

The simplified Chew-Pignotti model of Sec. III A generated a constant total cross section from a kernel $K(z)=e^{(2\alpha-1)z}$, with

$$B_a(y)=G_ae^y \quad \text{for } y\geq 0. \tag{3.27}$$

The production spectrum was rectangular with constant height and with a base of length Y:

$$\frac{d\sigma_{ab}}{dy}=G_ag^2G_b \quad \text{for} \quad 0\leq y\leq Y. \tag{3.28}$$

As the energy increased, the rectangle lengthened at a rate consistent with a logarithmic increase in multiplicity ($Y\approx\log s$).

If we suppose, however, that the model reproduces a more reasonable total cross section, the distribution is modified. At both ends of the distribution a resonance region occurs, which extends a finite distance towards the middle. At sufficiently high total energies a plateau develops in the middle. The plateau shrinks in height to a constant limit as the energy increases. For purposes of illustration let us suppose in the spirit of duality[24] that the resonance region is represented on the average by an extrapolation of two Regge-pole terms; i.e.,

$$B_a(y)\approx G_a(e^y+ce^{\alpha y}), \tag{3.29}$$

so that from (3.20),

$$\sigma_{ab}(Y)=G_aG_b[1+ce^{(\alpha-1)Y}]. \tag{3.30}$$

The distribution (3.26) is then of the form

$$\frac{d\sigma_{ab}}{dy}=G_ag^2G_b[1+c^2e^{(\alpha-1)Y}+ce^{(Y-y)(\alpha-1)}+ce^{y(\alpha-1)}]. \tag{3.31}$$

This distribution is illustrated in Fig. 4 for $c=1$, $G_ag^2G_b=1$, and $\alpha=0.5$. The first term represents the constant limit of the plateau, the second represents the shrinking component of the plateau, and the third and fourth cause the ends of the plateau to turn up. This distribution is evidently consistent with the

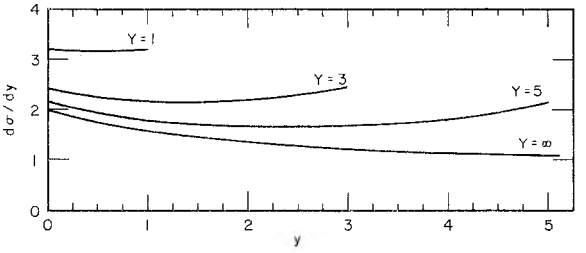

FIG. 4. Distribution in longitudinal momentum of produced secondaries in a simplified two-power model for $Y=1$, 3, 5, corresponding to proton beam energies 1.5, 9.3, 69.6 GeV, respectively; $d\sigma/dy$ has arbitrary units.

[22] In the simplified treatment of Sec. III we have omitted particles 0 and $n+1$, since they always appear at the elastic position in the strong-ordering limit. Hence the distributions which we obtain should be augmented by a δ function at both ends for these particles. The δ function has a weight equal to the total cross section.

[23] The expression (3.26) can be generalized in a rigorous treatment. See Refs. 7, 12, and 13 for details.

[24] G. F. Chew and A. Pignotti, Phys. Rev. Letters 20, 1078 (1968).

hypothesis of limiting fragmentation.[25] The distribution is symmetric under $y \to Y-y$. This result is a consequence of the simplicity of the model. In general the spectrum at the ends of the distribution differs depending on the incident particle at the end. The upward slopes at the ends can be made less prominent by decreasing the value of c.

A further consequence of this model is that the average multiplicity is no longer linear in log$s$. The slope in log$s$ decreases as log$s$ increases, and the curve approaches a straight line asymptotically. This result seems to be a general consequence of the two-power form for the total cross section, and was first discovered in the model of Chew and Snider.[5,26] The average multiplicity is obtained from (3.25) by integrating the distribution (3.31) over y and dividing by the total cross section (3.30). We find that

$$\langle n\rangle = g^2 Y + g^2 \frac{2c}{1-\alpha}\left\{\frac{1-e^{(\alpha-1)Y}}{1+c^2 e^{(\alpha-1)Y}}\right\}. \tag{3.32}$$

For large $Y \approx \log s$, the slope has the usual ABFST form. For small log$s$ the slope is related to the sum of the coefficients of the two powers in the total cross section, and for large log$s$, to the coefficient of the higher power,

$$\langle n\rangle \approx \begin{cases} g^2(1+c)Y & \text{for} \quad Y \to 0 \\ g^2\left(Y+\dfrac{2c}{1-\alpha}\right) & \text{for} \quad Y \to \infty . \end{cases} \tag{3.33}$$

The characteristic energy at which the multiplicity reverts to its asymptotic form may be found by equating the two expressions in (3.33). This yields $Y=2/(1-\alpha)$. If $\alpha=\frac{1}{2}$, this would imply that $s \approx m_a m_b e^4$, a rather low energy. Present experimental evidence for pp collisions[27] indicates an unchanging slope in log$s$ from accelerator energies up to cosmic-ray energies. Since the model of this section would, through its overly simplified factorization property, also make the prominently resonant πp cross section proportional to the obscurely resonant pp cross section, we are not particularly concerned with the difficulties in reproducing the experimental multiplicities with this model.

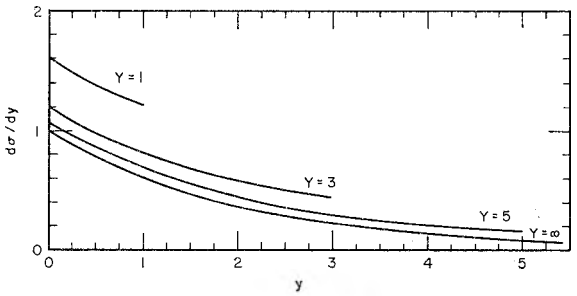

FIG. 5. Longitudinal momentum distribution of recoil proton in a simplified two-power model for $Y=1$, 3, 5, corresponding to proton beam energies 1.5, 9.3, 69.6 GeV, respectively; $d\sigma/dy$ has arbitrary units.

The presence of an upward slope at the ends of the spectrum implies a greater concentration of particles in this region. This would seem to contradict the expectation that the distribution in the subenergies, hence the interval between particles, should be the same anywhere in the chain in the strong-ordering limit. The paradox is resolved when one realizes that the particle at the end of the chain is rigidly fixed at the elastic position in the strong-ordering limit. The position in the spectrum of a given particle depends upon the accumulated intervals between particles up to the ends of the chain. If the distribution in subenergies has a suitable form (e.g., it has a two-power form) the average position of particles will not be uniform even if the average spacing is. We discuss below (Sec. IV) the consequences of incorporating a realistic elasticity.

C. Distribution of Final Baryons

The techniques of Sec. III B can be applied to a study of the spectrum of recoiling baryons. In the discussion so far, we have ignored distinctions between types of particles. The foregoing description applies best to meson-meson scattering, since most of the produced particles are observed to be mesons. It would also be applicable to the spectrum of produced particles in baryon-baryon scattering if we ignored those multiperipheral diagrams in which the baryons emerge at positions other than the ends of the chain. Caneschi and Pignotti have emphasized, however, that in a multi-Regge model, baryon exchange must occur for an average distance of a couple of links from the ends in order to reproduce the observed proton spectra at accelerator energies.[12] Following the model of Ting,[28] they obtained a fit to the data assuming that the baryon-antibaryon ladders build a trajectory with intercept $\alpha_A(0)=0.5$. The spectrum of recoiling protons may then be deduced from Eq. (3.26), if we stipulate that B_a be constructed strictly from baryon-antibaryon ladders. The function B_b should be the same as before, however. We then have

$$B_a(y) \approx G_a'' e^{\alpha_A(0)y}. \tag{3.34}$$

The target recoil distribution is illustrated in Fig. 5 for $\alpha_A(0)=0.5$ and with other parameters the same as in Fig. 4. Note that the distribution is concentrated at low values of y, as expected.

To obtain the spectrum for $pp \to p+$anything, one must, of course, add to the recoil spectrum in Fig. 5 the beam-scattering spectrum with $y \to Y-y$. In practice, the distribution should not shrink to zero in the middle,

[25] J. Benecke, T. T. Chou, C. N. Yang, and E. Yen, Phys. Rev. 188, 2159 (1969).
[26] Carleton E. DeTar and Dale R. Snider, Phys. Rev. Letters 25, 410 (1970).
[27] K. N. Erickson, University of Michigan, Ann Arbor report, 1970 (unpublished). See also Ref. 1 for multiplicities at accelerator energies.
[28] Peter Ting, Phys. Rev. 181, 1942 (1969).

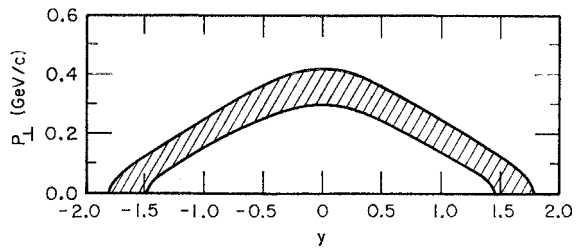

FIG. 6. Location of pions in the longitudinal boost plot, resulting from the decay of a ρ meson at $y=0$, $p_\perp=0$. The band corresponds to a mass width of 125 MeV.

because of the small, finite production of $p\bar{p}$ pairs. If we incorporated $p\bar{p}$ pair production into the model, the central part would gradually approach the spectrum for $pp\to\bar{p}+$anything, which in this simplified model conforms with Fig. 4.

D. Two-Particle Spectrum

Using arguments similar to those which led to Eq. (3.26), it is possible to show that the two-particle spectrum is simply

$$\frac{d^2\sigma_{ab}}{dy_1dy'}=e^{-Y}B_a(y)g^2C(y'-y)g^2B_b(Y-y') \quad (3.35)$$

for $y'\geq y$, where, formally,

$$C=K+Kg^2K+Kg^2Kg^2K+\cdots \quad (3.36)$$

is a ladder without "ends." The function C is simply related to B_a through the expression

$$B_a(Y)=G_aC(Y). \quad (3.37)$$

The double integral over the spectrum (3.35) yields $\langle n(n-1)/2\rangle\sigma_{ab}$. Combining this with the integral for $y'\leq y$, we obtain a net integral of $\langle n(n-1)\rangle\sigma_{ab}$, the expected result, since each contribution to the spectrum must be weighted by the number of ways two particles can be chosen from a multiplicity of n.

If C shows resonant structure, this is reflected in the correlation between particle momenta in the usual way. Measuring two-particle correlations is a particularly valuable technique for studying the kernel K. Note also that through (3.20) and (3.37), C has the same behavior at large Y as the total cross section, except for kinematic factors.

IV. REFINEMENTS

In the foregoing section we derived the secondary momentum distribution using a simplified model, in which transverse momenta were completely ignored and the particles were assumed to be strongly ordered. Among the features of these simplified distributions were (a) a plateau for the central part at high energies, (b) an upward slope away from the center at the ends, and (c) a sharp cutoff at the ends and a δ-function spike for the left-most and right-most particles on the chain.[22] In this section we estimate the modifications to these conclusions, which result from bringing the model more in accordance with reality.

It is not hard to show that the strong-ordering assumption for individual particles is poorly justified. Data[27] for the average multiplicity of secondaries per inelastic event in pp collisions at energies up to 880 GeV/c fit the expression $\langle n\rangle=a\ln s+b$ for $a=1.10$. In the model the distribution is of length $Y\approx\log s$. The particles are spaced uniformly in the center, so that an increase in Y of $\Delta y=1/a$ increases the average multiplicity by one. Therefore, the average spacing of particles in the center of the distribution in the variable y is $\langle\Delta y\rangle\approx 1$. If this spacing occurred as a rule, the strong-ordering assumption would be marginally correct. However, there is reason to expect a substantial spread in Δy, permitting "crossing" or negative values of Δy. In a comparison of the CŁA multiperipheral model with experimental data, Ajduk *et al.*[29] have shown that particles do tend to cross. It is easy to understand why, since they find that the average value of a $\pi\pi$ subenergy is about m_ρ^2. To estimate the spread in $|\Delta y|$, we consider the decay of a ρ meson, traveling along the z direction. The resultant distribution of pions in the space $p_\perp$, y is illustrated in Fig. 6. Note that $|\Delta y|$ ranges from 0 to about 3. The lower (negative) bound on Δy may be estimated from the peripheral constraint on the momentum transfers. Since [see Eq. (A9)]

$$t_i\approx -w_iw_{i+1}e^{-\Delta y_i}-(\sum_0^i \mathbf{p}_{\perp i})^2, \quad (4.1)$$

the more negative Δy, the larger the absolute value of t_i for a given set of transverse momenta. If the amplitude has an exponential cutoff for large t_i, and if $w_i\approx\bar{p}_{\perp i}\gg m_\pi$, a variation in Δy that doubled the magnitude of the first term would not reduce the amplitude severely. A value as low as -1 for Δy is not unexpected. Therefore, crossing between adjacent particles is rather common. The stronger the cutoff in t_i, the more rigorous the constraint from Eq. (4.1) becomes. The sharpest cutoff in t_i typically occurs for large values of $s_{i,i+1}$, i.e., large (positive) values of Δy_i, where this constraint does not operate. However, at moderate subenergies, we estimate there is frequent crossing in y. Of course, if the constraint imposed by (4.1) with an attenuation at large t_i is not sufficient, the particles can cross into a region of phase space where the amplitude for the new arrangement is large. If this overlap effect is important, it would appear to contradict the multiperipheral concept of a linear chain.

Many of these difficulties can be resolved if we follow the ABFST approach[7] and construct the chain from

[29] Z. Ajduk, L. Michejda, and W. Wójcik, Acta Phys. Polon. **A37**, 285 (1969). See also A. Jurewicz, L. Michejda, J. Namysłowski, and J. Turnau, in Proceedings of the Colloquium on High Multiplicity Hadronic Interactions, Paris, 1970 (unpublished), for a similar study with the ABFST model.

larger units. Suppose the units consist of two particles each. The analysis above is readily adapted to this model, if we treat pairs of particles formally as single decaying resonances. It is necessary to provide for variable masses, but the resultant distributions of di-particles is essentially the same as described in Sec. III. The average Δy between di-particles is then twice the average spacing between single particles, or $\langle\Delta y\rangle\approx 2$, and the effective lower bound on Δy from (4.1) is correspondingly higher for a given distribution in t_i, since w_i increases with the mass of the emitted "di-particle." Hence the ordering improves as the number of particles in the repeating unit is increased, thereby vindicating the concept of a linear chain.

One of the consequences of the strong-ordering assumption was that the end particles on the chain are produced as though the collision were elastic. Let us see how a model based on one- and two-particle units agrees with this hypothesis, given the empirical result that $\langle\Delta y\rangle\approx 1$ per particle.

From (A11) it is possible to estimate the average elasticity, if we assume that the transverse momenta are equal on the average:

$$\langle\eta_{b1}\rangle\approx(1+e^{-1}+e^{-2}+\cdots)^{-1}=1-1/e\approx 60\%. \quad (4.2)$$

Because of the considerable range of multiplicities (and the correspondingly large spread in Δy) the distribution in η_b is broad. However, the average elasticity in a di-particle model (defined as the fraction of the beam energy imparted to the most energetic di-particle) is considerably greater. Using the same methods, we find that with an average spacing $\langle\Delta y\rangle\approx 2$,

$$\langle\eta_{b2}\rangle\approx 1-1/e^2\approx 85\%. \quad (4.3)$$

Although we have assumed in keeping with experimental results that the distribution in transverse momentum is confined and small, it is interesting to speculate on the dynamical origins of this phenomenon. One factor which could constrain the value of the transverse momentum is a peripheral limitation on the momentum transfer. Referring again to Eq. (4.1), we see that if the distribution in t_i is governed by an exponential $\exp(bt)$, the distribution in $p_\perp^2$ would be, roughly speaking, $\exp(bp_\perp^2)$, if the $\mathbf{p}_{\perp j}$ were uncorrelated. However, other constraints could operate as well; for example, the presence of strong low-energy resonances (such as the ρ) help to confine the transverse momentum distribution. The ρ decays at rest into two pions with momentum 350 MeV/c. If the decay were isotropic, the average transverse momentum of the pions would be consistent with the observed average of about 400 MeV/c, if the average transverse momentum of the ρ were about 500 MeV/c, quite a reasonable value. The distribution in the transverse momentum reacts upon the distributions in the subenergies through kinematical constraints of the following type, which may be derived in the strong-ordering limit (see the Appendix):

$$s\approx(s_{01}s_{12}\cdots s_{n,n+1})/(w_1^2w_2^2\cdots w_n^2). \quad (4.4)$$

Generally speaking, the smaller the transverse momenta, the smaller the subenergies. Unfortunately, the subtleties of many-body kinematics prevent a more precise definition of the constraints upon the transverse momenta within the confines of a simple argument. We believe, however, that insofar as the transverse momenta are small compared with the masses of the particles, the results of the previous section are not substantially altered with the introduction of a finite transverse momentum. In particular, in a di-particle model, the masses exceed the typical transverse momenta.

If we suppose that the results of Sec. III are correct for a di-particle model, we can discover the sorts of features that a more realistic single-particle distribution should have, simply by convoluting the simplified distributions of Sec. III with the mass and decay spectrum of the di-particles. The resulting single-particle distributions will have the following general features: (a) a limiting form at high energies, (b) a flat distribution in y for the central part at high energies, (c) a smooth drop to zero at the ends over a typical range for a decaying resonance of $\Delta y\approx 1$ to 2. (Only the genuinely elastic events will contribute to the elastic spike.) It is possible, however, that the upward slope away from the center of the distribution of Eq. (3.31) will be washed out.

V. GENERAL DESCRIPTION OF SPECTRUM AND EXPERIMENTAL CONSEQUENCES

We are now in a position to formulate a general description of the single-particle production spectrum based on two assumptions: (a) that transverse momenta are limited and (b) that short-range order prevails along the multiperipheral chain.

We will argue that the "particle density" $(\sigma^{\text{tot}})^{-1}d^2\sigma/dydp_\perp$ is limiting in the sense of Yang and collaborators,[25] i.e., as the energy is increased, the low-lab-momentum part of the particle density approaches a constant function of $p_\perp$ and y, which depends only on the target and the observed particle, and the high-lab-momentum part of the particle density approaches a constant function of $p_\perp$ and $Y-y$, which depends only on the beam and the observed particle. Moreover, in the central part of the spectrum, a region $\Delta<y<Y-\Delta$ for some fixed Δ, the particle density is constant in y, depending only upon the observed particle. These conditions may be summarized by asserting that as the energy is increased, the spectrum of particle X in the process $a+b\to X+$anything approaches the form

$$(\sigma_{ab}{}^{\text{tot}})^{-1}\frac{d^2\sigma_{ab}{}^X}{dp_\perp dy}=\begin{cases}A_X(p_\perp,y) & \text{for } y<\Delta\\ f_X(p_\perp) & \text{for } \Delta<y<Y-\Delta\\ B_X(p_\perp,Y-y) & \text{for } Y<\Delta<y\end{cases} \quad (5.1)$$

for some fixed Δ.

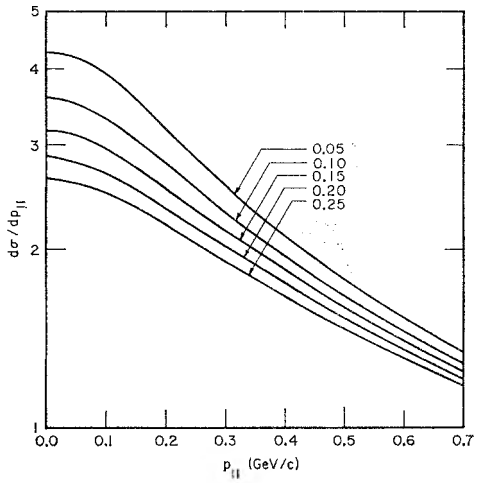

FIG. 7. The distribution $d\sigma/dp_{\parallel}$ for pions obtained by integrating $d\sigma/dp_{\perp}{}^2dp_{\parallel}=[E\langle p_{\perp}{}^2\rangle]^{-1}\exp(-p_{\perp}{}^2/\langle p_{\perp}\rangle^2)$ at fixed $p_{\parallel}$ for (top to bottom) $\langle p_{\perp}\rangle^2=0.05$, 0.10, 0.15, 0.20, and 0.25 $(\mathrm{GeV}/c)^2$.

We argue first that the particle density is limiting. Since particles that are distant in the sense of relative velocity are assumed to be uncorrelated, particles produced with small transverse momenta and $y<\Delta$ for some fixed Δ are correlated only with particles produced for a finite distance in y. In particular, at asymptotic energies the spectrum at $y<\Delta$ depends neither upon the chain length nor upon the beam particle, except by way of a normalization factor. The particle density in the variables y and $p_{\perp}$ is itself uncorrelated with the chain length and the beam particle, since the particle spacing in y and $p_{\perp}$ is determined by local correlations. Therefore the spectrum divided by the total cross section approaches a constant function of y and $p_{\perp}$ for $y<\Delta$ as the energy is increased, and this function depends only upon the target particle and the observed particle. An analogous argument holds for the other end of the spectrum with $y\rightarrow Y-y$.

Finally, we argue that for the central region of the spectrum $(\Delta<y<Y-\Delta)$ the particle density is constant in y, independent of the beam and target. More precisely, given an ϵ, there is a Y_0 and a Δ (which may depend on X), such that for $Y>Y_0$ and $\Delta<y<Y-\Delta$ the particle density is within a fraction ϵ of $f(p_{\perp})$. The result depends on the homogeneity of the central part of the multiperipheral chain, which can be viewed as a consequence of short-range order. Because any portion of the central region of the spectrum is generated by particles that decouple from remote parts of the multiperipheral chain, the spectrum in the central region must be independent of both beam and target, except for over-all normalization. Moreover, any two points at different values of y in the central region are equivalent with regard to factors that determine the spectra at these points. The particle spacings in $p_{\perp}$ and y depend only upon local correlations; and, insofar as any two points in the central region are equivalent in these correlations, the particle density is constant in y throughout the central region.[30]

It is tempting to identify the region $\Delta<y<Y-\Delta$ with the pionization component and the rest of the spectrum with the components of beam and target fragmentation in the language of Yang and collaborators, although the components merge with one another in a continuous fashion. If pionization in this sense were absent, then $f_X(p_{\perp})=0$, and the production of particle X would be connected in some way with the particular choice of beam or target. It is possible to construct a multiperipheral model for which this would occur. Imagine a model for $pp\rightarrow p+$anything that did not include the possibility of producing $p\bar{p}$ pairs. The observed protons would then correspond to the persisting baryons at the ends of the chain. In practical models, it may even be desirable to ignore small production rates of this sort. However, in principle, it is plausible to expect that the production of an arbitrary number of pairs $X\bar{X}$ occurs whenever sufficient energy is available. In terms of the multiperipheral model this possibility is realized by allowing the production of any pair $X\bar{X}$ in the repeating portion of the chain. Assuming this indefinite proliferation of particles, it follows that f_X is nonvanishing and that the average multiplicity of particle X is linear in $\ln s$ at asymptotic energies. The coefficient of $\ln s$ is given by

$$g_X=\int f_X(p_{\perp})dp_{\perp} \tag{5.2}$$

and the relative probability for producing various particles is given by the relative values of g_X. A recent experiment at cosmic-ray energies[27] gives $g_{\pi^{\pm}}\approx\frac{2}{3}$, a value which Bali *et al.*[17] find to be in quite good agreement with the central part of the particle density for pions in present experiments (see below). This is strong evidence for the presence of pionization.

A model with limiting fragmentation, but without pionization would develop a zero in the center of the distribution. The fragmentation components would approach zero at large distances in y from the respective ends. Under these conditions, the average multiplicity would necessarily grow less rapidly than $\log s$.

If f_X is nonvanishing, and if for asymptotic Y,

$$\sigma_{ab}{}^{\mathrm{tot}}(Y)\sim G_aG_be^{\alpha Y} \tag{5.3}$$

(the latter follows from all known multiperipheral models), one can then recast (5.1) in a language strongly reminiscent of Feynman's:

$$\frac{d^2\sigma_{ab}{}^X}{dp_{\perp}dy}\sim A_X'(p_{\perp},y)B_X'(p_{\perp},Y-y), \tag{5.4}$$

[30] To say that all points in the central region are equivalent is only approximately correct. As we noted in Sec. III it is conceivable that the spectrum, when restricted to events of a given multiplicity, could be periodic in y. Strictly speaking, we cannot rule out the possibility that the net inclusive spectrum has some fine structure, but any fluctuations will occur about a constant average. It is in this sense that we speak of a flat distribution.

where A' is related to the probability for finding a parton in particle a with coordinates $p_\perp$ and y and B' is the analogous probability for particle b. Moreover, both $A_X'(p_\perp,y)$ and $B_X'(p_\perp,y)$ have the power behavior $e^{\alpha y}$ for asymptotic y. Putting $\alpha=0$ gives Feynman's result that the production cross section is limiting and that the central part is constant in y.

There are several simple but important consequences of the result (5.1) which should be emphasized here.

1. In all longitudinally moving frames, in which particles with $p_{11}\approx 0$ come from the central portion of the chain, there will be a peak in the distribution of the form $dp_\perp dp_{11}/E$ at $p_{11}=0$. The experimental results reported by Erwin[31] show a peak in $d\sigma/dp_{11}$ at $p_{11}=0$ in several longitudinally moving frames.

2. The distribution $d\sigma/dy$ obtained by integrating over $p_\perp$ at fixed y develops a constant plateau in y which elongates with energy. However, the shape of the peak at $p_{11}=0$ in the distribution $d\sigma/dp_{11}$ obtained by integrating over $p_\perp$ at fixed p_{11} depends upon the form of the distribution in transverse momentum. In Fig. 7 we show the distribution $d\sigma/dp_{11}$ obtained when $d^2\sigma/dp_\perp{}^2dp_{11}=(E\langle p_\perp{}^2\rangle)^{-1}\exp(-p_\perp{}^2/\langle p_\perp{}^2\rangle)$ for various choices of $\langle p_\perp{}^2\rangle$.

3. The angular distribution in any longitudinally moving frame, $d\sigma/d\cos\theta$, has a forward and backward peak, whenever particles from the central part of the chain can move in these directions. The exact shape depends, of course, on the distribution in transverse momentum and the spectrum from the ends of the chain. This follows from the approximate identification $y\approx\ln(2/\tan\theta)$ for $p_{11}\gg p_\perp\gtrsim m$. Hence $dy\approx d\cos\theta/\sin^2\theta$ for $|\sin\theta|\ll 1$.

4. The Duller-Walker plot[32] (the logarithm of the ratio of the forward to backward fraction vs log $\tan\theta$) shows a "break" at the center, which has been used[33] as partial evidence for the two-fireball model. The forward/backward fraction $F/(1-F)$ is simply $y/(Y-y)$ for the flat part of the distribution. The resulting Duller-Walker plot is shown in Fig. 8.

5. Bali *et al.*[17] relate the height of the distribution in the center to the coefficient of ln$s$ in the expression for the average multiplicity. With the distribution (5.1), this is simply expressed as follows: If the total cross section is constant, and the distribution has reached its limiting form, then $\langle n_X\rangle\sim g_X\ln s+\text{const}$, where $\langle n_X\rangle$ is the average multiplicity of particle X per event. The constant g_X is given by (5.2) and is independent of beam or target.

There remain several questions, which can not be answered except within the context of a specific model. Some of these questions are: (a) At what energy does the plateau in $d\sigma/dy$ begin to develop? (b) Does the plateau slope upwards from the center at either end of the distribution; i.e., is the plateau in a valley? (c) Given that the total cross section approaches a constant, how rapidly is the limiting distribution reached? (d) What is the limiting shape of the distribution?

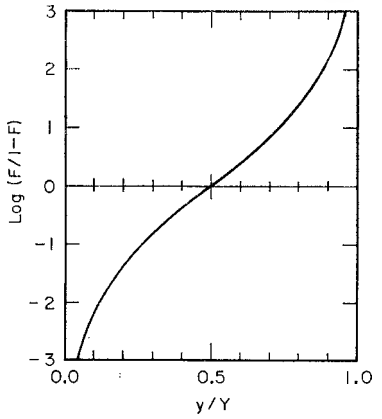

FIG. 8. Duller-Walker plot for the longitudinally invariant distribution, $\log_{10}[F/(1-F)]$ vs y/Y, where y is linearly related to $\log_{10}\tan\theta$.

To stimulate experimental interest in these questions, we will venture a guess at the answer to the first one. In a sense, the answer depends on the assumed effective correlation length and the density of particles at the ends of the distribution. Let us assume that it is permissible to neglect correlations that involve more than two particles, though it is important to represent the two-particle resonance region correctly, and furthermore, that the strong-ordering approximation is marginally acceptable for pairs of particles. Because the ρ resonance is prominent in the $\pi\pi$ cross section and the Δ in the πp cross section, we would then expect that as the total energy was increased, a plateau would begin to develop in the pion spectrum from $\pi p\to\pi+$anything after the process $\pi p\to\rho\Delta$ represented a significant fraction of the inelastic cross section. At what energies does this occur? Experimentally, it is observed that the process $\pi^+p\to\Delta^{++}\rho^0$ accounts for $\frac{1}{4}$ to $\frac{1}{3}$ of the events $\pi^+p\to p\pi^+\pi^+\pi^-$ at energies in the range 3–8 GeV/c.[34] The four-body process $\pi^-p\to p\pi^+\pi^-\pi^-$ represents a significant fraction of the inelastic cross section up to about 10 GeV/c.[35] This would suggest that one should look for the plateau above 10 GeV/c. For $pp\to\pi+$anything the characteristic process would be $pp\to\Delta\Delta$. The cross section for $pp\to\Delta^{++}\Delta^0$ peaks strongly in the region 5–7 GeV/c.[36] This gives one indication of the energy beyond which one should look for the plateau.

[31] A. R. Erwin, "Multiparticle Production—Experimental," presented at the Conference on Expectations for Particle Reactions at the New Accelerators, Madison, Wisconsin, 1970 (unpublished).

[32] N. M. Duller and W. D. Walker, Phys. Rev. **93**, 215 (1954).

[33] Giuseppe Cocconi, Phys. Rev. **111**, 1699 (1958).

[34] G. Goldhaber *et al.*, Phys. Rev. Letters **12**, 336 (1965); Aachen-Berlin-Birmingham-Bonn-Hamburg-London (I.C.)-München Collaboration, Phys. Rev. **138B**, 897 (1965); P. Slattery *et al.*, Nuovo Cimento **50A**, 377 (1967); ABC Collaboration: M. Deutschmann *et al.*, Phys. Letters **19**, 608 (1965).

[35] ABBCCHW Collaboration: R. Hönecker *et al.*, Nucl. Phys. **B13**, 571 (1969).

[36] R. Panvini, in *High Energy Collisions* (Gordon and Breach, New York, 1969), p. 497.

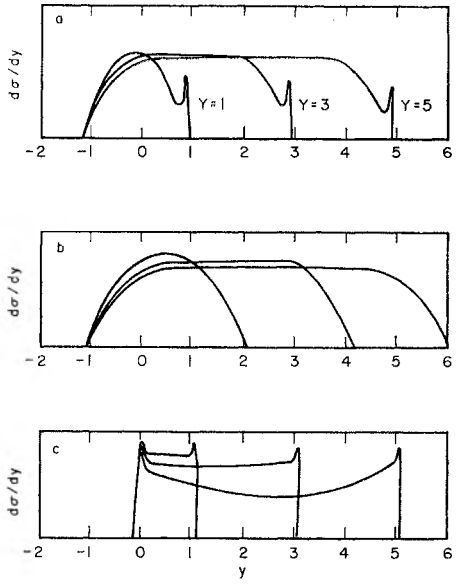

FIG. 9. Sketch of the longitudinal momentum distribution $d\sigma/dy$ of secondaries predicted in the multiperipheral model, showing the evolution with increasing energy, $Y=1$, 3, 5. The spikes represent the elastic scattering events. (a) $\pi p \to \pi$+anything; (b) $pp \to \pi$+anything; (c) $pp \to p$+anything.

We obtain another estimate by comparing the πp reaction with the pp reaction. For a comparable-sized plateau, the spacing in the y variable between the ρ and Δ should be the same as between the Δ and Δ. Since $s_{pp} \approx m_\Delta m_\Delta e^{\Delta y}$, the spacing is the same, if $s_{\pi p} \approx m_\rho m_\Delta e^{\Delta y}$. Hence for $p_{\text{lab},\pi}=10$ GeV/c, $p_{\text{lab},p} \approx 15$ GeV/c. Combining our estimates, we suggest that for π beam momenta above about 5–10 GeV/c and p beam momenta above about 7–15 GeV/c one should begin to expect a plateau.

In Fig. 9 we present freehand sketches of the evolution with energy of the spectra $d\sigma/dy$ for the following reactions exhibiting the general features which we have identified in the analysis above:

(a) $\pi p \to \pi$+anything,
(b) $pp \to \pi$+anything,
(c) $pp \to p$+anything.

What is the experimental evidence for this description? In the past few months considerable evidence has accumulated in support of limiting fragmentation. In addition to evidence presented by Yang and collaborators[25] and Smith,[37] the recent work of Vander Velde[38] and Bali *et al.*,[17] examining experimental data for $pp \to \pi^\pm$+anything and $pp \to p$+anything, also indicates that a significant part of the spectrum approaches a limit at accelerator energies. Bali *et al.* studied the spectra in the variables x and $p_\perp$. They fitted data for $\pi^\pm$ at 12.2,[39] 19.2,[40] and 30 GeV/c[41] to the expression

$$\frac{d\sigma}{dp_\perp^2 dp_{\parallel}} = \frac{\pi}{E} F(p_\perp)G(x) \qquad (5.5)$$

and found agreement among individual points within factors of 1.5 or better. We translated their fitted expression at 30 GeV/c into the variables $p_\perp$ and y and present in Fig. 10 the resultant spectrum $d\sigma/dy$, obtained by integrating over $p_\perp$ at fixed y. Strictly speaking, only three points on this curve are determined by the experiment of Anderson *et al.*[41] at 30 GeV/c, since the experiment was carried out at three laboratory angles, which correspond essentially to three values of y through the relation $y-Y \approx \ln(\frac{1}{2}\tan\theta)$. These points are indicated in Fig. 10. However, the curve is qualitatively similar to those obtained at lower energies. In general, therefore, there seems to be some evidence that limiting fragmentation occurs at accelerator energies, and that there is a tendency for the spectrum to level off as y increases. If we accept the evidence for limiting fragmentation, then the observation[27] that the average multiplicity is linear in $\ln s$ implies that the central part of the spectrum is constant. Bali *et al.* noted that at 30 GeV/c the height of the spectrum at $x=0$ ($y=2.1$) is within 10% of what would be expected from the rate of increase of $\langle n \rangle$ with $\ln s$ at cosmic-ray energies. This would suggest that the spectrum has attained the height of the plateau in Fig. 10 and that this height should prevail between the points $y \approx 2$ and $y \approx Y-2$ as the energy is increased.

We join Bali *et al.* in urging that experiments be carried out for a larger range of laboratory angles to

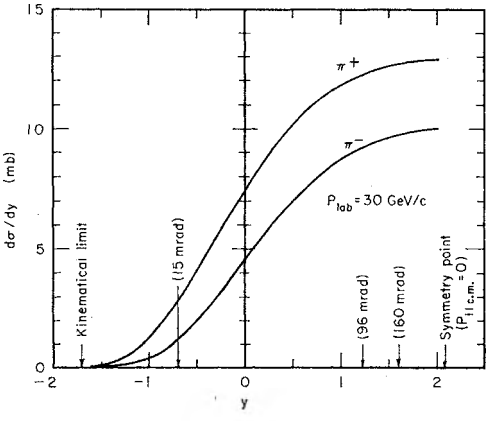

FIG. 10. The low-y portion of the spectrum $d\sigma/dy$ for $pp \to \pi^\pm$ +anything at 30 GeV/c derived from the fitted formula of Bali *et al.* (Ref. 17). Shown are the three points in y where the data of Anderson *et al.* (Ref. 41) are concentrated.

[37] Dennis B. Smith presented data for the reaction $pp \to \pi^-$+ anything at various energies, and showed that the low-energy part of the distribution in the lab system was remarkably constant as a function of beam momentum [Bull. Am. Phys. Soc. **15**, 659 (1970)].

[38] J. C. Vander Velde, University of Michigan, Ann Arbor report, 1970 (unpublished).

[39] J. L. Day, *et al.*, Phys. Rev. Letters **23**, 1055 (1969).

[40] J. W. Allaby *et al.*, CERN Report No. 70-12, 1970 (unpublished).

[41] E. W. Anderson *et al.*, Phys. Rev. Letters **19**, 198 (1967).

test limiting fragmentation, and, in particular, near $p_{\parallel \text{c.m.}}=0$ to investigate the development of the plateau.

VI. COMPARISON WITH OTHER MODELS

A. Two-Fireball Model

Although there is presumably considerable leeway for modifying the two-fireball model, inasmuch as it is basically phenomenological, we will use the model as proposed by Cocconi[33] for the purposes of comparison. In this model a collision between two hadrons, viewed in the center-of-mass system, is supposed to result in two persisting hadrons with momenta reduced by a fraction, which is fixed on the average, and two fireballs, which decay after separating relatively slowly from the point of collision along the incident directions. The decay is thought to be isotropic in the center-of-mass system of the fireball with secondary energies fixed on the average, so that the transverse momentum does not increase with the total energy.

With such a model, it is impossible to obtain a nontrivial limiting distribution for the contribution to the momentum spectrum from the fireballs and still have increasing multiplicities. Suppose that in the center-of-mass system, the fireball associated with the target particle moves with velocity $\beta_{F,\text{c.m.}}$. Then the energy of the fireball in the center-of-mass system is

$$E_{F,\text{c.m.}}=\gamma_{F,\text{c.m.}}M_F=\gamma_{F,\text{c.m.}}\bar{E}n_F=\kappa E_{0,\text{c.m.}}, \quad (6.1)$$

where M_F is the fireball mass, $\bar{E}$ is the fixed average energy of the decay products, n_F is the average multiplicity of the decay, κ is the inelasticity, and $E_{0,\text{c.m.}}$ is the energy of the target particle in the center-of-mass system. Since $E_{0,\text{c.m.}}=\gamma_{\text{c.m.}}m_a$, where m_a is the mass of the target particle, we conclude that

$$n_F=2\kappa m_a\gamma_{F,\text{lab}}/\bar{E}, \quad (6.2)$$

since $\gamma_{\text{c.m.}}\approx 2\gamma_{F,\text{c.m.}}\gamma_{F,\text{lab}}$. (In terms of the longitudinal boost variables, $\gamma_{F,\text{lab}}=\cosh y_F$.) Equation (6.2) shows that, if the average multiplicity increases, the velocity of the fireball in the laboratory frame also increases. The center of the decay spectrum of the fireball must then shift to the right in y. Since the energy $\bar{E}$ is fixed, the spectrum in y will not increase in width as it shifts, only in height. The spectrum in $p_{\parallel\text{lab}}$ will also shift to higher values of the momentum; hence, the distribution is clearly not limiting except in a trivial sense. This behavior is sketched in Fig. 11.

Another quite obvious feature of the momentum spectrum in the fireball model is the presence of a distinct dip in the center of the spectrum in y, reflecting the distinguished role of the center-of-mass frame.

Actually, the multiperipheral model does permit individual events to have fireball-like features. In collaboration with Snider,[26] the author has studied various multiperipheral mechanisms, which could produce gaps in the spectrum for individual events. It was found that substantial gaps could occur; but, because they could occur at any point in the spectrum, the average spectrum had no gaps or pronounced dips.

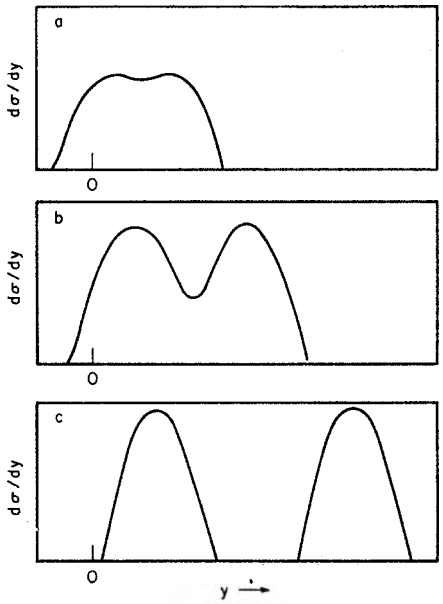

FIG. 11. Sketch of the longitudinal momentum distribution $d\sigma/dy$ of secondaries predicted in the two-fireball model, showing evolution with increasing energy a, b, and c.

B. Isobar-Pionization Model

The isobar-plus-pionization model in its purest form[42] is orthogonal to the two-fireball model in that it predicts not a dip, but a peak in the center of the spectrum $d\sigma/dy$, which comes from the pionization component. Nevertheless, there is practically a continuous gradation of models between this model and the two-fireball model.[43] The model was originally proposed by Pal and Peters to explain the unexpectedly large momenta of some secondaries. Viewed in the center-of-mass system, the collision of two hadrons is thought to result in excited states of the hadrons (isobars), moving along the incident directions, which carry off a substantial fraction of the energy, and a cloud of mesons. The meson cloud decays according to a fixed isotropic distribution (perhaps with some anisotropy favoring the forward-backward directions) in the center-of-mass system, the secondaries carrying a fixed energy on the average.[42]

The decay of the isobars could be brought into accordance with the hypothesis of limiting fragmentation, since the model is flexible on this point. The pionization component is not limiting as long as its decay distribution remains fixed in the center-of-mass system. It

[42] Yash Pal and B. Peters, Kgl. Danske Videnskab. Selskab, Mat.-Fys. Medd. **33**, No. 15 (1964).

[43] M. Koshiba, in *High Energy Collisions* (Gordon and Breach, New York, 1969), p. 161.

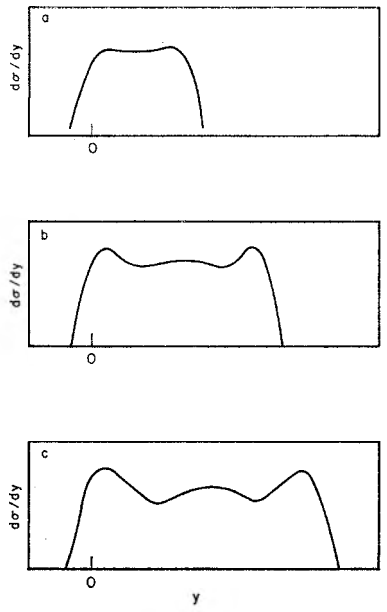

FIG. 12. Sketch of the longitudinal momentum distribution $d\sigma/dy$ of secondaries predicted in the isobar-pionization model with a limiting distribution for the isobar component.

contributes a peak in $d\sigma/dy$ which shifts to the right with increasing energy, as shown in the sketch in Fig. 12.

If distinct dips are seen in the experimental spectrum between the "isobar" and "pionization" contribution, then the isobar-pionization model would definitely be confirmed. Otherwise, a prominent central hump in the distribution, which persisted to high energies, would be strongly supportive. Some recently proposed models with extreme forward-backward anisotropy in the center-of-mass system actually predict a central dip,[44] however, and it is conceivable that with clever manipulation, it should be possible to imitate the predictions of the multiperipheral model for a finite range of total energies.

One of the applications of the isobar-pionization model has been an attempt to understand the propagation of the high-energy component of cosmic-ray secondaries through the atmosphere, since the selection of certain prominent isobars implies a definite population of energetic decay products.[42] In particular, the model could explain the observed excess of positive to negative high-energy muons in cosmic-ray showers. Koshiba has applied the model with great zeal to a study of the population ratio of low-energy pions to kaons in cosmic-ray events observed in emulsions.[43] (These would come from the decay of the recoiling target isobar.)

Limiting fragmentation alone could provide a valuable tool for clarifying these questions. Rather than assuming *ad hoc* that certain isobars are present, one could simply extend the observed ratios of π^+/π^- and π/K at accelerator energies to cosmic-ray energies for the corresponding part of the secondary spectrum. Except for the parameter that marks the separation between the limited and nonlimited part of the spectrum, the extrapolation would be parameter-free and the predictions would provide a test of limiting fragmentation.

[44] The distribution $a+b\cos^n\theta$ for the pionization component (see Ref. 44) can be made to produce a dip in the log $\tan\theta$ plot if a/b is sufficiently small and n sufficiently large.

C. Statistical Thermodynamical Model

The model of Hagedorn and Ranft[45] describes the single-particle spectrum in terms of a local statistical distribution

$$f(\epsilon',T)\propto\frac{d^3p'}{e^{\epsilon'/kT}\pm1}, \tag{6.3}$$

where $\epsilon'=[(p')^2+m^2]^{1/2}$, and a function which specifies the collective longitudinal motion of the hadronic "fluid," $F(\lambda)$, where

$$\lambda=\pm\frac{\gamma-1}{\gamma_0-1}=\pm\frac{\cosh(y-\frac{1}{2}Y)-1}{\cosh\frac{1}{2}Y-1}. \tag{6.4}$$

The parameter λ defines a longitudinal boost $(y-\frac{1}{2}Y)$, which relates the center-of-mass frame to the local rest frame in which a portion of the fluid decays according to the distribution (6.3). The sign of λ specifies the direction of the boost. The spectrum for producing one particle X in conjunction with anything else is then obtained by convoluting the distribution (6.3) with a longitudinal Lorentz transformation $L(\lambda)$ according to the weight function $F(\lambda)$,

$$\frac{d\sigma_X}{dp_{\parallel}dp_{\perp}}=Q_X(E_0)\int_{-1}^{1}d\lambda\,F_X(\lambda)L(\lambda)f(\epsilon_X',T(\lambda)), \tag{6.5}$$

where E_0 is the beam energy. Depending upon the particle type, different expressions appear in place of $F(\lambda)$, according to the specifications of the model. The expressions all have in common an energy independence, and the form of F is determined phenomenologically. The normalization Q depends upon the particle type and is in principle determined by the model, but in current practice from the data. It is allowed to vary with energy. The variation usually amounts to factors of 1.5 to 2. This is partly a consequence of systematic errors in the data. The temperature T is a function of λ, but for most of the range of λ, varies slowly around a value of $0.8\,T_0$, where $T_0=160$ MeV.

Since the distribution $f(\epsilon,T)$ is peaked for small local momenta, the longitudinal momentum distribution is, roughly speaking, described by $F(\lambda)$:

$$dN/d\lambda\approx QF(\lambda)\,. \tag{6.6}$$

[45] We discuss the latest published version of the model, as it applies to the production spectrum: R. Hagedorn and J. Ranft, Nuovo Cimento Suppl. 6, 169 (1968); see also R. Hagedorn, *ibid.* 56A, 1027 (1968).

For $e^{|y-Y/2|}\gg 1$ and $e^{Y/2}\gg 1$,

$$\lambda=(m_a/w)x=\begin{cases} e^{(y-Y)} \\ -e^{y}, \end{cases} \tag{6.7}$$

where x is the Feynman parameter [see (2.7)]. Therefore, for fixed x (or fixed y or $Y-y$) and sufficiently large energies, the distribution is a fixed function of x (or y or $Y-y$), provided Q approaches a constant. Hence, the distribution is limiting,[46] if Q is constant.[47]

Is it possible to choose a form for $F(\lambda)$ so that the central part of the distribution is invariant under longitudinal boosts?[48] To obtain an invariant distribution we require that

$$\begin{aligned} &T(\lambda)=\text{const}, \\ &F(\lambda)d\lambda=dy \quad \text{for } |\lambda|<\lambda_0 \end{aligned} \tag{6.8}$$

for some constant λ_0. From Eq. (6.4) this implies that

$$F(\lambda)=\lambda^{-1}(1+2e^{-Y/2}/\lambda)^{-1/2}, \tag{6.9}$$

which depends on Y as well as λ. Thus it is impossible for a fixed function of λ to give an invariant distribution in the same sense as the multiperipheral model. If we choose

$$F(\lambda)=1/\lambda, \tag{6.10}$$

as suggested by Ranft and Ranft,[48] the distribution is eventually invariant for $s^{1/2}/2m=e^{Y/2}\gg\lambda^{-1}$, for any fixed nonzero λ, whereas one would expect a much more uniformly limiting distribution in the multiperipheral model.

As in the case of the Feynman variable x, the difficulty lies in the choice of variable. If a closer correspondence between the multiperipheral model and the statistical thermodynamical model were desired, one might use the variable y in place of λ so that Eq. (6.5) would read

$$\frac{d^2N}{dp_{\parallel}dp_{\perp}}=\int_0^Y dy\,F(Y,y)L(y)f(\epsilon',T). \tag{6.11}$$

For not too small λ, the change in variable is trivial,

$$F(Y,y)=|\lambda|F(\lambda) \quad \text{for } |\lambda|\gg e^{-Y/2}=2ms^{-1/2}, \tag{6.12}$$

with λ given by (6.7). The present fits to experimental data can be used to construct the function $F(Y,y)$. Since these were obtained with pp collisions up to 30 GeV/c, the lower bound on $|\lambda|$ in (6.12) is at least 0.25. This function should be comparable to the distribution $d\sigma_{ab}/dy$ in (3.26) and is limiting in the same sense, i.e., it may be written as

$$F(Y,y)=A(y)B(Y-y), \tag{6.13}$$

where both A and B have a constant limit in y as $y\to\infty$. The condition (6.13) replaces the requirement that F be independent of energy. If $A\propto B$, then F is symmetric under $y\to Y-y$. We have taken the function $F(\lambda)$, given by Ranft and Ranft,

$$F(\lambda)\propto(1-|\lambda|)e^{-a|\lambda|}$$

with $a=5.13$ and constructed the function $F(Y,y)$ for $0\leq y\leq 2$, which corresponds roughly to $-1\leq\lambda\leq-0.15$. The result is plotted in Fig. 13. Evidently it exhibits some of the qualitative features of Fig. 10, even though the functions are indirectly related through Eq. (6.11). The function $F(Y,y)$ rises over a region in y of $\Delta y\approx 2$ and begins to level off. It is tempting to take this as evidence for the onset of a plateau (or a downward slope to a flat valley), but in view of the aforementioned complications in interpreting distributions at small values of λ, and because of limitations in the data, we cannot draw a definite conclusion from this result.

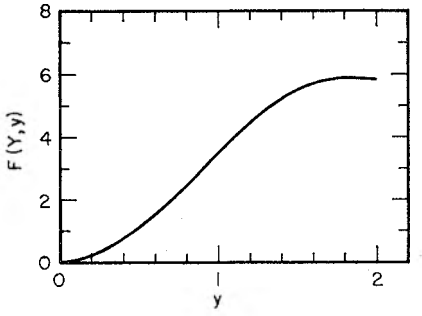

FIG. 13. The low-y portion of the Lorentz boost weight function $F(y,Y)$ in the statistical thermodynamical model. The vertical scale is in arbitrary units.

In summary, the statistical thermodynamical model in its present form is not entirely compatible with the multiperipheral model, but with a slight modification (6.11) can be brought into accordance with it. Its chief distinctive feature is a characteristic distribution in transverse momentum, given by $f(\epsilon,T)$. The success of the fits of Hagedorn and Ranft[46,49] to a broad collection of single-particle production spectra can be understood largely as a demonstration that limiting fragmentation is valid at accelerator energies to within normalization factors of 1.5 to 2. It seems that the predominant experimental support for the model amounts to little more than this. In any case proponents of limiting fragmentation will undoubtedly find the phenomenological expressions of Hagedorn and Ranft to be a useful summary of the data.

[46] Liland and Pilkuhn state that the statistical thermodynamical model does not "scale": A. Liland and H. Pilkuhn, Phys. Letters **29B**, 663 (1969). However, their scaling is not the same as limiting fragmentation. Therefore there is no contradiction here. See Vander Velde (Ref. 38) for a discussion of this point.

[47] Hagedorn has also discussed this point. See R. Hagedorn, Nucl. Phys. **B24**, 93 (1970).

[48] Ranft and Ranft have considered this question. See G. Ranft and J. Ranft, Phys. Letters **32B**, 207 (1970).

[49] J. Ranft, Rutherford Laboratory Report No. RHEL/R165, 1968 (unpublished); Phys. Letters **31B**, 529 (1970).

D. Conclusion

In their description of the single-particle distribution, three current models of multiparticle production, the multiperipheral model with a constant total cross section, the Feynman parton model, and the liquid droplet model (as understood by Cheng and Wu[50]) are in agreement. This poses some interesting theoretical questions about the similarities among the models. The perturbation diagrams which Cheng and Wu have studied to support their intuitive conclusions[50] do seem to satisfy our criteria of a multiperipheral model—namely, factorization (short-range order) and small transverse momenta. However, it is difficult to determine from its published form[15] whether the parton model fulfills these criteria.

Experimenters who enjoy resolving intense theoretical controversy will doubtless find such unanimity rather disappointing. Nevertheless (even though they are outnumbered), the isobar-pionization and two-fireball models do give rather different predictions. If limiting fragmentation continues to hold true, the two-fireball model is in trouble, and if a central plateau in the distribution $d\sigma/dy$ is observed, the multiperipheral model, the parton model, and the liquid-droplet model would be strongly supported.

ACKNOWLEDGMENTS

I am indebted to Dale Snider and Dennis B. Smith for many stimulating conversations. I am deeply grateful to Geoffrey Chew for his continuing inspiration and guidance throughout my graduate career.

APPENDIX

We derive here the relationship between the conventional Lorentz invariants and the longitudinal boost variables, and obtain some expressions required in the text.

Let us define the subenergy

$$s_{i,i+1}=(P_i+P_{i+1})^2, \tag{A1}$$

the cluster energy

$$s_{0,i}=(\sum_{j=0}^{i} P_j)^2, \tag{A2}$$

and the momentum transfer

$$t_i=(\sum_{j=0}^{i} P_j-P_a)^2. \tag{A3}$$

If we write the Lorentz scalar product consistently as

$$P^2=(P_t-P_z)(P_t+P_z)-\mathbf{p}_\perp^2 \tag{A4}$$

and use the definitions (2.2), we easily obtain the following expressions:

$$s_{i,i+1}=2w_iw_{i+1}\cosh(y_i-y_{i+1})+m_i^2+m_{i+1}^2-2\mathbf{p}_{\perp i}\cdot\mathbf{p}_{\perp i+1},$$

$$s_{0,i}=[\sum_{j=0}^{i} w_je^{y_j}][\sum_{j=0}^{i} w_je^{-y_j}]-(\sum_{j=0}^{i}\mathbf{p}_{\perp j})^2, \tag{A5}$$

$$t_i=[\sum_{j=0}^{i} w_je^{y_j}-m_a][\sum_{j=0}^{i} w_je^{-y_j}-m_a]-(\sum_{j=0}^{i}\mathbf{p}_{\perp j})^2.$$

If we use the conservation constraint given by the second δ function in (2.3) we can rewrite the last expression:

$$t_i=-[\sum_{j=0}^{i} w_je^{y_j}-m_a][\sum_{j=i+1}^{n+1} w_je^{-y_j}-m_be^{-Y}] -(\sum_{j=0}^{i}\mathbf{p}_{\perp j})^2. \tag{A6}$$

In the strong-ordering limit $y_i\ll y_{i+1}$, the expressions then become

$$s_{i,i+1}\approx w_iw_{i+1}e^{y_{i+1}-y_i}, \tag{A7}$$

$$s_{0,i}\approx w_0w_ie^{y_i-y_0}, \tag{A8}$$

$$t_i\approx -w_iw_{i+1}e^{y_i-y_{i+1}}-(\sum_{j=0}^{i}\mathbf{p}_{\perp j})^2. \tag{A9}$$

If particle $n+1$ is the persisting counterpart of particle b, the elasticity is defined to be

$$\eta_b=E_{n+1}/E_b. \tag{A10}$$

From (2.2) and the first conservation constraint in (2.3) we obtain

$$\eta_b\approx[1+(w_n/w_{n+1})e^{y_n-y_{n+1}} +(w_{n-1}/w_{n+1})e^{y_{n-1}-y_{n+1}}+\cdots]^{-1}. \tag{A11}$$

In the strong-ordering limit, energy-momentum conservation is expressed by the δ function in (3.6). In terms of the definitions (3.4) and (3.5) and the relation (2.5), we have

$$Y=x_a+z_1+z_2+\cdots+z_{n+1}+x_b, \tag{A12}$$

or

$$\ln\left(\frac{s}{m_am_b}\right)=\ln\left(\frac{w_0}{m_a}\right)+\ln\left(\frac{s_{01}}{w_0w_1}\right)+\ln\left(\frac{s_{12}}{w_1w_2}\right)+\cdots +\ln\left(\frac{s_{n,n+1}}{w_nw_{n+1}}\right)+\ln\left(\frac{w_{n+1}}{m_b}\right). \tag{A13}$$

Therefore

$$s=(s_{01}s_{12}\cdots s_{n,n+1})/(w_1^2w_2^2\cdots w_n^2), \tag{A14}$$

an expression analogous to one given by Chew and Pignotti.

[50] Hung Cheng and Tai Tsun Wu, Phys. Rev. Letters **23**, 1311 (1969).